

12 June 1964

RADIATION RESEARCH ASSOCIATES, INC.

Fort Worth, Texas

A MONTE CARLO STUDY OF THE TRANSPORT OF NEUTRONS RESULTING FROM PROTON-INDUCED NUCLEAR EVAPORATION

M. B. WELLS

R

	OTS PRICE
XEROX	\$ <u>2.65 ph</u>
MICROFILM	\$ _____

FACILITY FORM 602	N 64 28934	
	(ACCESSION NUMBER)	(THRU)
	<u>30</u>	<u>1</u>
	(PAGES)	(CODE)
	CR 58493	<u>23</u>
	(NASA CR OR TMX OR AD NUMBER)	(CATEGORY)

Work Performed For

GEORGE C. MARSHALL SPACE FLIGHT CENTER

Under Contract NAS8-11047

RRR-20178

RRA-M43
12 June 1964

A MONTE CARLO STUDY OF THE TRANSPORT
OF NEUTRONS RESULTING FROM PROTON-INDUCED
NUCLEAR EVAPORATION

M. B. Wells

Paper to be Presented at the
1964 Annual Meeting of the
American Nuclear Society
(Philadelphia, Pa., June 14-17, 1964)

Work Supported by the George C. Marshall Space
Flight Center, National Aeronautics and Space Administration,
Huntsville, Alabama under Contract NAS8-11047

RADIATION RESEARCH ASSOCIATES, INC.
Fort Worth, Texas

ABSTRACT

Monte Carlo methods are being used in performing a parameter study of the transport of neutrons through slabs of aluminum, polyethylene, carbon, and iron for use in further machine calculations of the neutron dose in space vehicles which results from proton-induced nuclear evaporation. The calculations being performed are for plane isotropic monoenergetic neutron sources located at various depths within a slab shield. The source plane locations and source energies were selected so that data for slabs of up to 30 cm thick and source energies between 0.5 Mev and 14 Mev could be obtained by interpolation from the Monte Carlo calculations.

The results obtained to date are mainly from aluminum, and show that the amount by which the boundary effects influence the dose rate transmitted through slabs is highly dependent on both the location of the plane isotropic source within the slab and the slab thickness. Differences of as much as a factor of 3 in the transmitted dose rate are noted between the slab results and similar calculations for a plane isotropic source in an infinite medium.

Author

INTRODUCTION

During recent years the transport of secondary neutrons produced in proton shields has been investigated in order to determine the importance of this component for space radiation shielding. The dose due to proton-induced evaporation neutrons at shield thickness Z is usually given by the equation

$$D(Z) = \int_0^Z T(Z-Z') S(Z') dZ'$$

where $S(Z')$ is the evaporation neutron source term at position Z' and $T(Z-Z')$ is the dose transmission function. Even with the assumption that evaporation neutrons are emitted isotropically with a fission neutron spectrum there is very little data available giving the transmission function $T(Z-Z')$ for plane sources located within a finite slab. Moments method data are available for a few elements and compounds¹; however, these data apply only to an infinite homogeneous medium so that heterogeneous slab configurations and boundary effects are not taken into account properly. Monte Carlo data are also available for a few elements and compounds^{2,3,4,5}; but these data also are not available for slab compositions and boundary conditions of interest.

In order to provide data on neutron dose transmission which takes into account boundary effects, a parameter study is currently being conducted on the transport of neutrons from monoenergetic plane isotropic sources embedded in slabs of aluminum, carbon, polyethylene, and iron that range in thickness from 1 to 30 cm.

The neutron transmission calculations are being performed on Monte Carlo codes developed for both slab and infinite medium geometries^{6,7}. The results obtained to date are mainly for aluminum. The fast neutron cross sections

used in the Monte Carlo calculations for aluminum were taken from compilations^{8,9} prepared by United Nuclear Corporation. A search of the literature revealed that there were no data available for point and plane isotropic mono-energetic sources in an infinite homogeneous medium of aluminum, therefore, calculations for these geometries were performed so that comparisons could be made with the results of the slab problems.

METHODS

The C18 Monte Carlo slab penetration code⁶ is being used to compute the transmission of monoenergetic neutrons emitted by a plane isotropic monoenergetic source located within a slab of finite thickness. The normal thickness of a slab in centimeters is denoted as Z . For each slab thickness, problems were run for each of six source locations: $0.01Z$, $0.19Z$, $0.39Z$, $0.59Z$, $0.79Z$, and $0.99Z$. The use of these source locations allows one to obtain, by interpolation of the Monte Carlo calculations, data for other source locations. The source energies being used in the C18 Monte Carlo calculations were chosen to represent important segments of the evaporation neutron spectrum. The slab thicknesses used in the calculations were selected to represent slab thicknesses within the range $1 \leq Z \leq 30$ cm. The factors being used to convert neutron flux to RBE tissue dose rate were obtained from the data reported by Henderson¹⁰. The neutron energy below which neutron histories are terminated is 0.2 Mev.

The results being obtained from the slab calculations are: 1) the angular distribution of the transmitted fast-neutron dose rate, 2) the energy and spatial distribution of the neutron flux within the slab, and 3) the spatial distribution of the dose rate within the slab.

Calculations are also being performed using the K74 Monte Carlo Code⁷ to determine the fast-neutron dose rate as a function of distance R and angle from point isotropic monoenergetic sources in infinite homogeneous media. The results are used as the attenuation kernel $G(R, E_0)$ in a FORTRAN program which converts the point isotropic source calculation to that for a plane isotropic source by evaluating the integral:

$$T(Z, E_0) = \int_0^{\pi/2} \frac{G(Z \sec \theta, E_0)}{\cos \theta} d(\cos \theta)$$

in which $Z \sec \theta$ corresponds to R . The quantity $T(Z, E_0)$ is the fast-neutron dose rate in an infinite homogeneous medium at a distance Z from a plane isotropic source emitting neutrons of energy E_0 .

The dose rates $G(R, E_0)$ were adjusted by use of the calculated angular distribution of the dose rate in the infinite homogeneous media to obtain a modified attenuation kernel, $G'(R, E_0)$, for use in calculations of the dose rate at a material-vacuum interface located Z centimeters from a plane isotropic source in a semi-infinite medium. In these calculations, the integral

$$T'(Z, E_0) = \int_0^{\pi/2} \frac{G'(Z \sec \theta, E_0)}{\cos \theta} d(\cos \theta)$$

was evaluated by the use of a FORTRAN Program. The quantity $T'(Z, E_0)$ is an approximation of the dose rate at the material-vacuum interface of a semi-infinite medium where the interface is located Z centimeters from a plane isotropic source parallel to the boundary. Comparison of the quantities $T(Z, E_0)$ and $T'(Z, E_0)$ shows the effects of plane boundaries on neutron dose rate transmission through slab shields.

RESULTS

Figure 1 shows the variation of the fast-neutron dose rate transmitted through aluminum slabs with source energy for several slab thicknesses Z where the source in all problems was a plane isotropic source located $0.99 Z$ cm from the exit face of each slab. It is seen that the dose rate transmitted through a slab of given thickness increases rapidly with increasing source energy for source energies between 0.5 and 2 Mev. For source energies greater than 2 Mev the dose rates for a given slab thickness level off and show a gradual increase with increasing source energy up to 8 Mev.

Figure 2 presents transmitted dose rates from a 4 Mev plane isotropic source as a function of source position in aluminum slabs ranging in thickness from 2 to 30 centimeters. The effect of holding the source position constant and increasing the slab thickness behind the source plane may be seen in this figure. It shows that for a source plane located at a fixed distance from the exit face of the slab, the transmitted dose rate increases to a maximum as the slab thickness is increased from 0 to 10 centimeters behind the slab. These results clearly indicate that the transmitted dose rate for a plane isotropic source located a fixed distance from a slab boundary is highly dependent on the slab thickness Z .

Table I contains a tabulation of the results of the Monte Carlo calculations giving the fast-neutron dose rate transmitted through aluminum slabs of various thicknesses for plane isotropic monoenergetic sources with energies of 0.5, 1, 2, 3, 4, 6, and 8 Mev. The source planes were located at distances within each slab of $0.01Z$, $0.19Z$, $0.39Z$, $0.59Z$, $0.79Z$, and $0.99Z$, where Z is the slab thickness in centimeters. From an examination of the data given in Table I for the transmitted dose rate from a plane isotropic source located at $0.99Z$ cm inside the slab it is seen that for a given energy, the transmitted dose rate increases with increasing slab

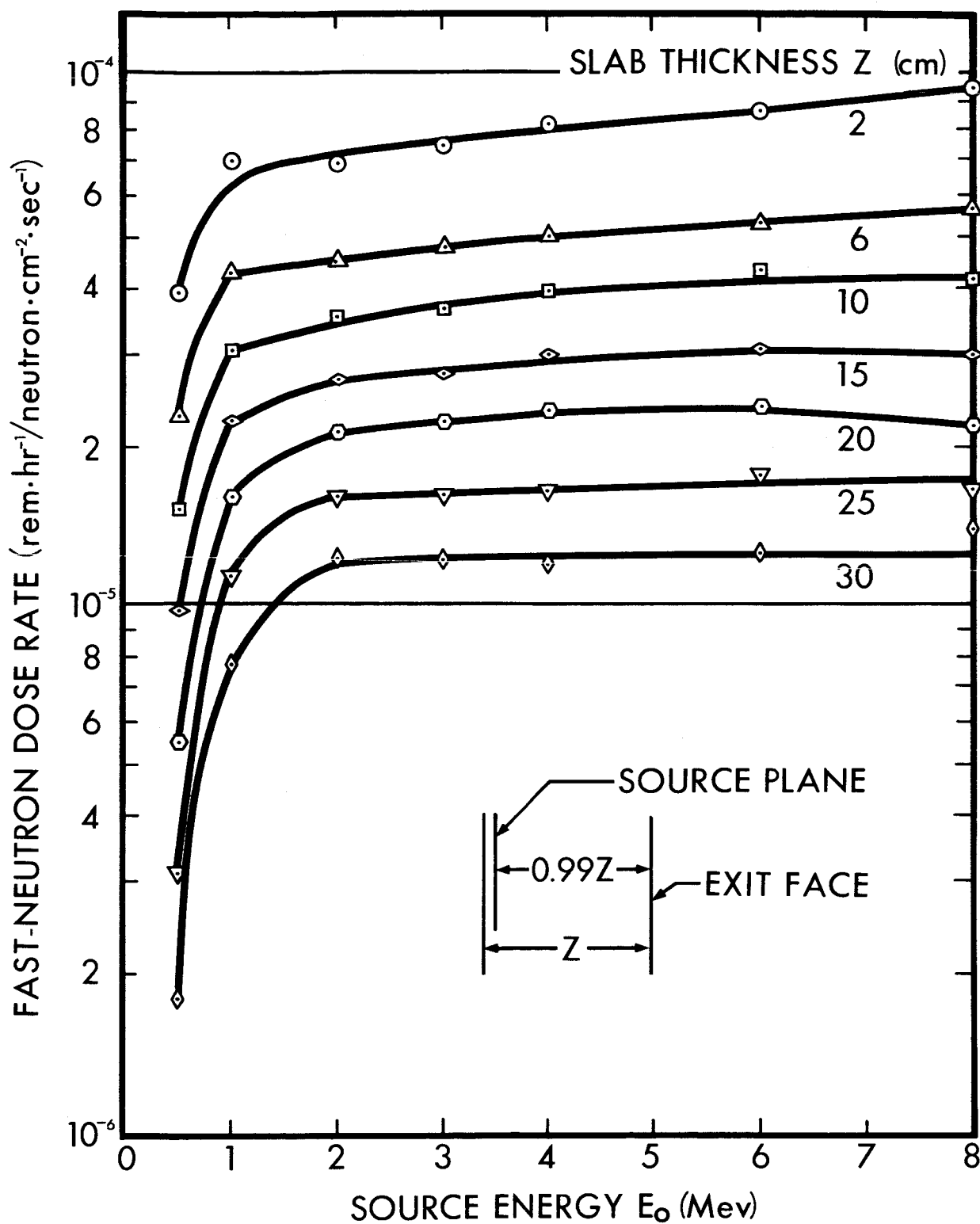


Figure 1. FAST-NEUTRON DOSE RATE TRANSMISSION THROUGH ALUMINUM SLABS VS. E₀

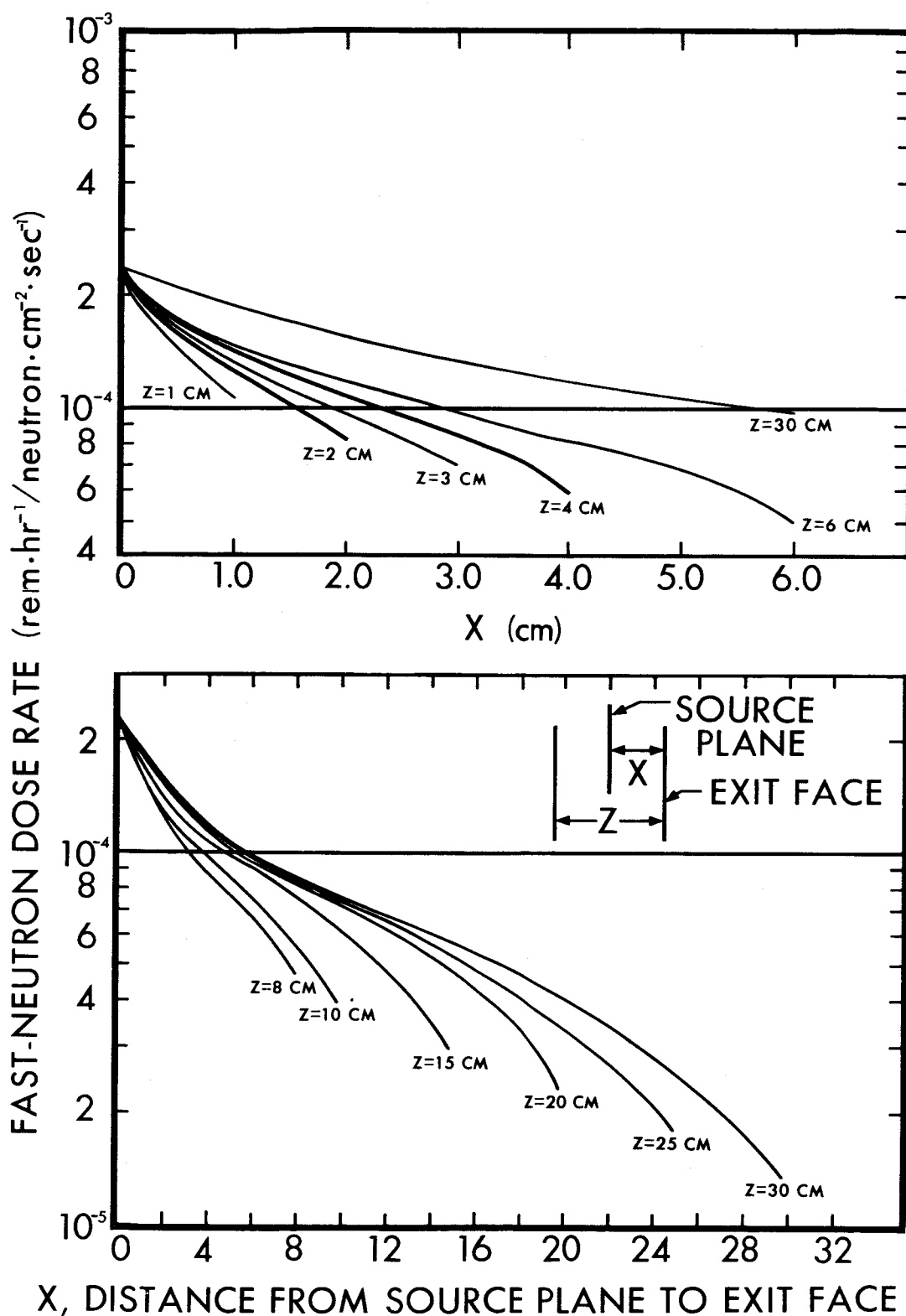


Figure 2. FAST-NEUTRON DOSE RATE TRANSMISSION THROUGH ALUMINUM SLABS AS A FUNCTION OF SOURCE LOCATION: 4 Mev PLANE ISOTROPIC SOURCE

Table I.

FAST NEUTRON DOSE TRANSMISSION THROUGH ALUMINUM SLABS FOR PLANE ISOTROPIC SOURCES IMBEDDED
WITHIN SLABS OF VARIOUS THICKNESSES

(rem·hr⁻¹/neutron·cm⁻²·sec⁻¹)

Source Energy (Mev)	Slab Thickness Z (cm)	Source Location at iZcm From Exit Face				
		i=0.01	i=0.19	i=0.39	i=0.59	i=0.79
0.5	1	.559-4	.603-4	.712-4	.834-4	.953-4
	2	.394-4	.502-4	.586-4	.726-4	.911-4
	3	.336-4	.432-4	.535-4	.650-4	.850-4
	4	.295-4	.373-4	.486-4	.604-4	.799-4
	6	.231-4	.328-4	.441-4	.573-4	.756-4
	8	.176-4	.284-4	.401-4	.516-4	.699-4
	10	.154-4	.248-4	.366-4	.499-4	.654-4
	15	.982-5	.178-4	.285-4	.402-4	.606-4
	18	.702-5	.141-4	.238-4	.376-4	.561-4
	20	.558-5	.124-4	.212-4	.335-4	.531-4
	25	.311-5	.758-5	.153-4	.274-4	.487-4
	30	.180-5	.480-5	.109-4	.215-4	.416-4
	1	.924-4	.100-3	.116-3	.136-3	.154-3
	2	.708-4	.816-4	.991-4	.114-3	.144-3
	3	.571-4	.726-4	.864-4	.105-3	.132-3
1.0	4	.514-4	.654-4	.791-4	.989-4	.123-3
	6	.435-4	.547-4	.707-4	.891-4	.116-3
	8	.359-4	.528-4	.663-4	.816-4	.111-3
	10	.309-4	.454-4	.616-4	.801-4	.104-3
	15	.225-4	.380-4	.546-4	.731-4	.980-4
	18	.192-4	.336-4	.492-4	.680-4	.931-4
	20	.163-4	.313-4	.458-4	.654-4	.929-4
	25	.117-4	.230-4	.371-4	.584-4	.849-4
	30	.780-5	.185-4	.314-4	.492-4	.790-4
	1					.123-3
	2					.127-3
	3					.133-3
	4					.133-3
	6					.128-3
	8					.132-3
	10					.134-3
	15					.131-3
	18					.126-3
	20					.125-3
	25					.122-3
	30					.118-3
	1					.191-3
	2					.195-3
	3					.202-3
	4					.192-3
	6					.200-3
	8					.198-3
	10					.197-3
	15					.196-3
	18					.194-3
	20					.187-3
	25					.190-3
	30					.189-3

Read .559-4 as 0.599x10-4

Table I., Continued.

(rem·hr⁻¹/neutron·cm⁻²·sec⁻¹)

Source Energy (Mev)	Slab Thickness Z (cm)	Source Location at iZcm From Exit Face					
		i=0.01	i=0.19	i=0.39	i=0.59	i=0.79	i=0.99
2.0	1	.911-4	.101-3	.123-3	.135-3	.160-3	.193-3
	2	.694-4	.875-4	.102-3	.120-3	.147-3	.203-3
	3	.627-4	.776-4	.903-4	.115-3	.143-3	.2-1-3
	4	.547-4	.715-4	.833-4	.105-3	.135-3	.217-3
	6	.453-4	.635-4	.804-4	.970-4	.128-3	.207-3
	8	.394-4	.579-4	.738-4	.943-4	.120-3	.215-3
	10	.355-4	.526-4	.735-4	.914-4	.114-3	.213-3
	15	.271-4	.451-4	.657-4	.829-4	.114-3	.213-3
	18	.227-4	.407-4	.607-4	.825-4	.107-3	.209-3
	20	.215-4	.396-4	.559-4	.796-4	.105-3	.204-3
	25	.163-4	.332-4	.516-4	.707-4	.100-3	.201-3
	30	.125-4	.273-4	.436-4	.657-4	.942-4	.201-3
	1	.973-4	.107-4	.118-3	.140-3	.158-3	.199-3
	2	.751-4	.899-4	.104-3	.124-3	.150-3	.201-3
	3	.636-4	.785-4	.946-4	.115-3	.143-3	.200-3
3.0	4	.569-4	.729-4	.878-4	.106-3	.134-3	.209-3
	6	.482-4	.618-4	.795-4	.964-4	.124-3	.207-3
	8	.420-4	.590-4	.756-4	.929-4	.124-3	.218-3
	10	.367-4	.542-4	.709-4	.915-4	.116-3	.207-3
	15	.276-4	.466-4	.620-4	.833-4	.109-3	.216-3
	18	.240-4	.415-4	.620-4	.785-4	.107-3	.210-3
	20	.215-4	.405-4	.571-4	.785-4	.104-3	.210-3
	25	.176-4	.345-4	.533-4	.728-4	.101-3	.210-3
	30	.136-4	.295-4	.455-4	.685-4	.962-4	.201-3

Table I., Continued

(rem·hr⁻¹/neutron·cm⁻²·sec⁻¹)

Source Energy (Mev)	Slab Thickness Z (cm)	Source Location at iZcm					
		i=0.01	i=0.19	i=0.39	i=0.59	i=0.79	i=0.99
4.0	1	.108-3	.119-3	.131-3	.157-3	.177-3	.214-3
	2	.824-4	.978-4	.114-3	.136-3	.163-3	.222-3
	3	.710-4	.845-4	.103-3	.121-3	.156-3	.225-3
	4	.601-4	.801-4	.941-4	.118-3	.151-3	.230-3
	6	.508-4	.709-4	.859-4	.109-3	.135-3	.223-3
	8	.471-4	.627-4	.796-4	.970-4	.132-3	.230-3
	10	.399-4	.545-4	.757-4	.967-4	.125-3	.235-3
	15	.300-4	.464-4	.674-4	.900-4	.116-3	.223-3
	18	.264-4	.425-4	.615-4	.846-4	.114-3	.228-3
	20	.234-4	.412-4	.600-4	.796-4	.113-3	.228-3
	25	.185-4	.347-4	.500-4	.748-4	.105-3	.221-3
	30	.132-4	.273-4	.460-4	.659-4	.989-4	.214-3
	1	.116-3	.125-3	.143-3	.165-3	.180-3	.212-3
	2	.870-4	.103-3	.121-3	.142-3	.173-3	.232-3
	3	.753-4	.891-4	.108-3	.123-3	.162-3	.229-3
	4	.652-4	.830-4	.998-4	.120-3	.156-3	.222-3
	6	.536-4	.705-4	.846-4	.109-3	.139-3	.237-3
	8	.475-4	.625-4	.799-4	.101-3	.134-3	.228-3
6.0	10	.435-4	.556-4	.730-4	.919-4	.126-3	.227-3
	15	.288-4	.478-4	.636-4	.877-4	.117-3	.236-3
	18	.258-4	.403-4	.596-4	.814-4	.112-3	.236-3
	20	.230-4	.373-4	.559-4	.781-4	.111-3	.232-3
	25	.178-4	.318-4	.490-4	.717-4	.101-3	.228-3
	30	.127-4	.252-4	.444-4	.644-4	.952-4	.222-3

Table I., Continued

(rem·hr⁻¹/neutron·cm⁻²·sec⁻¹)

Source Energy (Mev)	Slab Thickness Z (cm)	Source Location at iZcm From Exit Face					
		i=0.01	i=0.19	i=0.39	i=0.59	i=0.79	i=0.99
8.0	1	.126-3	.138-3	.151-3	.167-3	.190-3	.231-3
	2	.954-4	.112-3	.130-3	.152-3	.173-3	.227-3
	3	.792-4	.970-4	.111-3	.131-3	.166-3	.238-3
	4	.700-4	.847-4	.104-3	.126-3	.157-3	.239-3
	6	.563-4	.706-4	.880-4	.109-3	.145-3	.234-3
	8	.465-4	.625-4	.792-4	.102-3	.135-3	.239-3
	10	.410-4	.562-4	.722-4	.939-4	.124-3	.234-3
	15	.298-4	.456-4	.604-4	.838-4	.113-3	.234-3
	18	.257-4	.385-4	.557-4	.758-4	.110-3	.230-3
	20	.220-4	.372-4	.523-4	.724-4	.106-3	.233-3
	25	.166-4	.296-4	.472-4	.652-4	.965-4	.229-3
	30	.140-4	.243-4	.395-4	.575-4	.880-4	.225-3

thickness up to about 10 cm where a decrease with increasing slab thickness is noted. This decrease results from the fact that the distance at which the source plane is located from the slab face increases as the slab thickness increases. The attenuation of the direct beam for a source location at 0.99Z cm increases with increasing slab thickness Z. This increase in attenuation of the direct beam results in a slight decrease in the transmitted dose rate for Z greater than 10 cm since the scattered dose rate does not appear to increase as the slab thickness is increased beyond 10 cm.

The angular distributions ($\text{rem}\cdot\text{hr}\cdot\text{steradian}/\text{neutron}\cdot\text{cm}^{-2}\cdot\text{sec}^{-1}$) of the transmitted fast-neutron dose rate through aluminum slabs of various thicknesses are shown in Figure 3, where θ is the angle between the direction of the transmitted dose rate and a normal to the slab surface. It is noted that for slab thicknesses of 6 cm or less the shapes of the angular distributions do not vary rapidly with increasing Z. The shape of the angular distributions for slab thickness greater than 6 cm changes slowly with increasing thicknesses up to about 10 cm. For thicknesses of 10 cm and more the shapes of the angular distributions do not change with increasing thickness. The shape of the distributions for $\theta > 20^\circ$ and Z = 10, 15, 20, and 30 cm can be described fairly well by a $\cos^{1.5} \theta$ distribution.

The angular distribution of the transmitted fast-neutron dose rate for a source plane located 6 cm from the exit face is shown as a function of the slab thickness in Figure 4. There is little difference noted in the shapes of the distributions as a function of slab thickness, but there is a considerable difference in the magnitude of the dose rate. The transmitted dose rate increases rapidly as the slab thickness behind the source plane increases from 0 to 10 cm. As the slab thickness behind the source increases beyond 10 cm there is little difference noted in the magnitude of the transmitted dose rate.

The spatial distribution of the fast neutron fluxes within a 30 cm thick

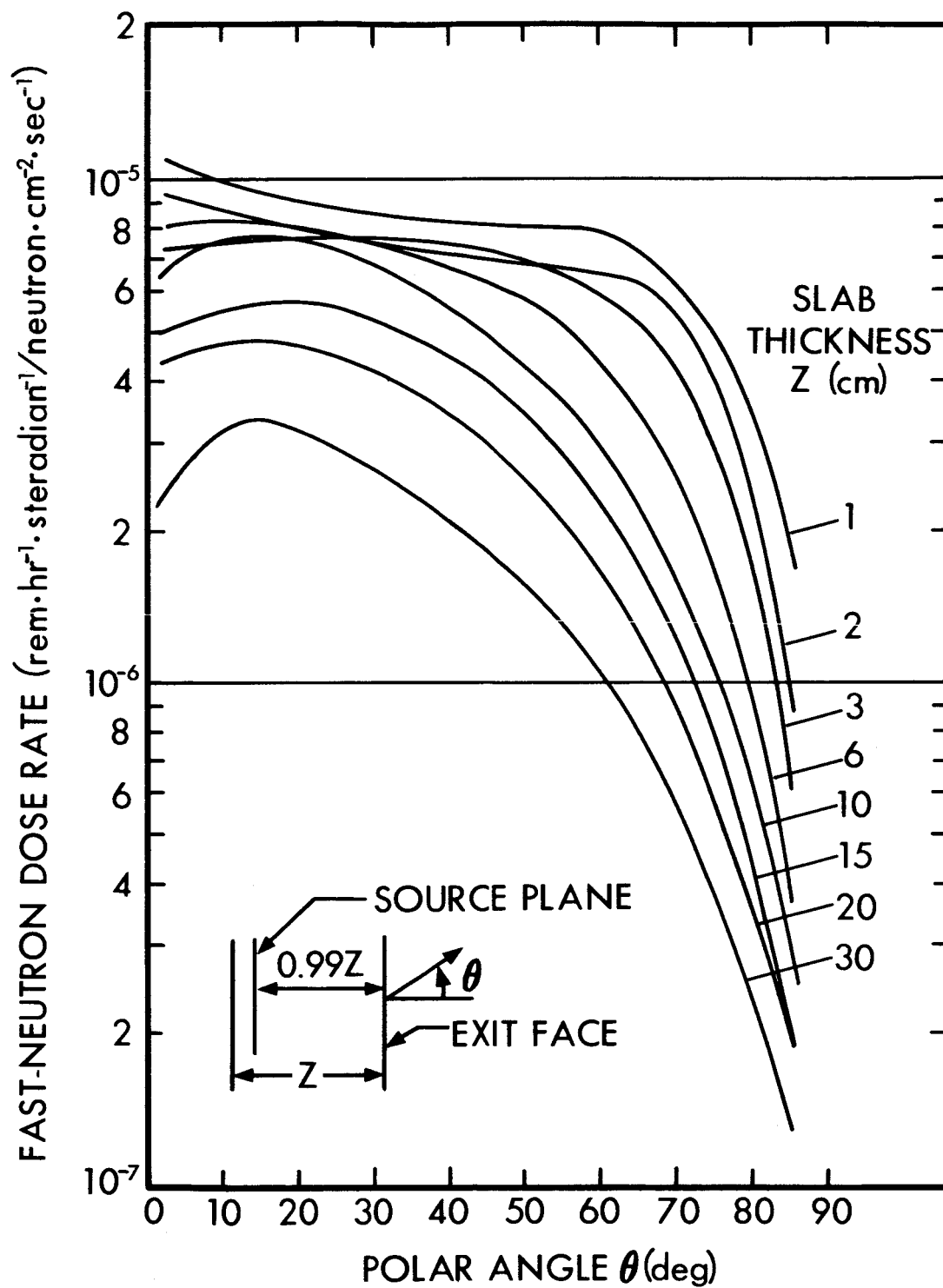


Figure 3. ANGULAR DISTRIBUTION OF THE FAST-NEUTRON DOSE RATE TRANSMITTED THROUGH ALUMINUM SLABS OF VARIOUS THICKNESSES: 3 Mev PLANE ISOTROPIC SOURCE

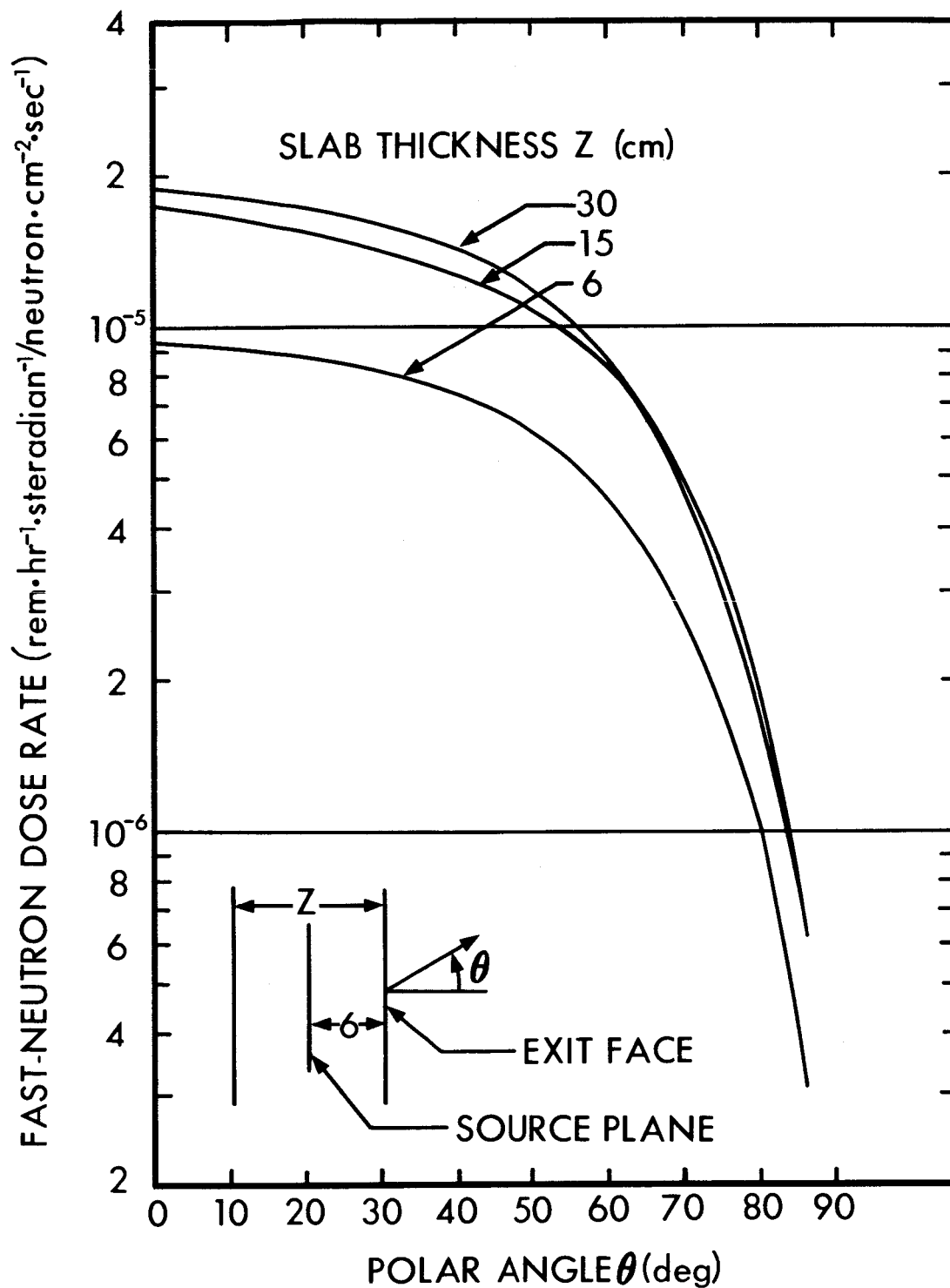


Figure 4. ANGULAR DISTRIBUTION OF THE FAST-NEUTRON DOSE RATE TRANSMITTED THROUGH 6 CM OF ALUMINUM AS A FUNCTION OF SLAB THICKNESS: 4 Mev PLANE ISOTROPIC SOURCE

aluminum slab is presented in Figure 5 as a function of energy for the case where a 6 Mev plane isotropic source is located at one face of the slab. The direct beam flux, as expected, falls off more rapidly with distance from the source plane than the fluxes in any of the energy intervals indicated. It is noted that the magnitude of the neutron fluxes decreases with decreasing energy for neutron energies between 6 and 3.68 Mev. For neutron energies between 3.68 and 0.2 Mev the magnitude of the fluxes increases with decreasing energy. It is also noted that the spatial distributions of the fluxes in the energy intervals indicated fall off less rapidly with increasing distance from the source plane as the neutron energy decreases in magnitude.

The effect of slab thickness on the neutron energy spectrum at a distance of 15 cm from a 6 Mev plane isotropic source located on one face of both a 15 and 30 cm thick aluminum slab is shown in Figure 6. It is seen that the thickness of the aluminum beyond the detector plane has little effect on the neutron fluxes above 5 Mev. The contribution to the flux at 15 cm from the source plane by neutrons reflected from the material beyond the detector plane is seen to be quite large for scattered neutron energies below 5 Mev.

Most machine programs that have been developed for the purpose of computing the radiation field inside a specified space vehicle compartment have made use of infinite medium dose transmission data in evaluating the dose resulting from the production and transmission of proton-induced evaporation neutrons. Therefore, it is instructive to see how the slab results for neutrons differ from the results obtained from calculations of neutron transport in both infinite and semi-infinite medium geometries.

The variation of the fast-neutron dose rate with distance from a 6 Mev plane isotropic source for both an infinite homogeneous medium of aluminum and a semi-infinite medium of aluminum is seen in Figure 7. The neutron dose rate in the

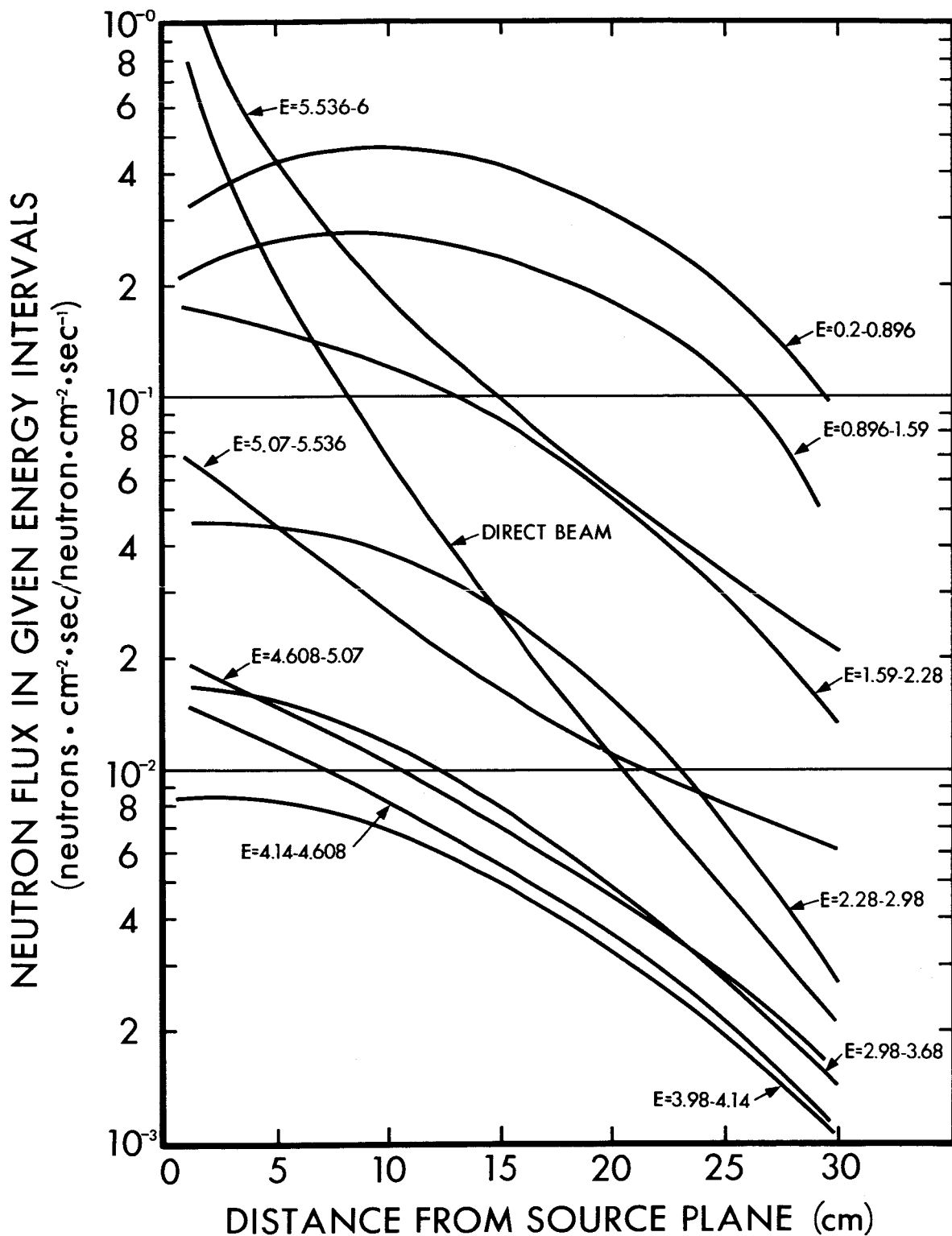


Figure 5. NEUTRON FLUX AS A FUNCTION OF DISTANCE AND ENERGY WITHIN A 30 CM ALUMINUM SLAB: 6 Mev PLANE ISOTROPIC SOURCE LOCATED 0.6 CM INSIDE SLAB

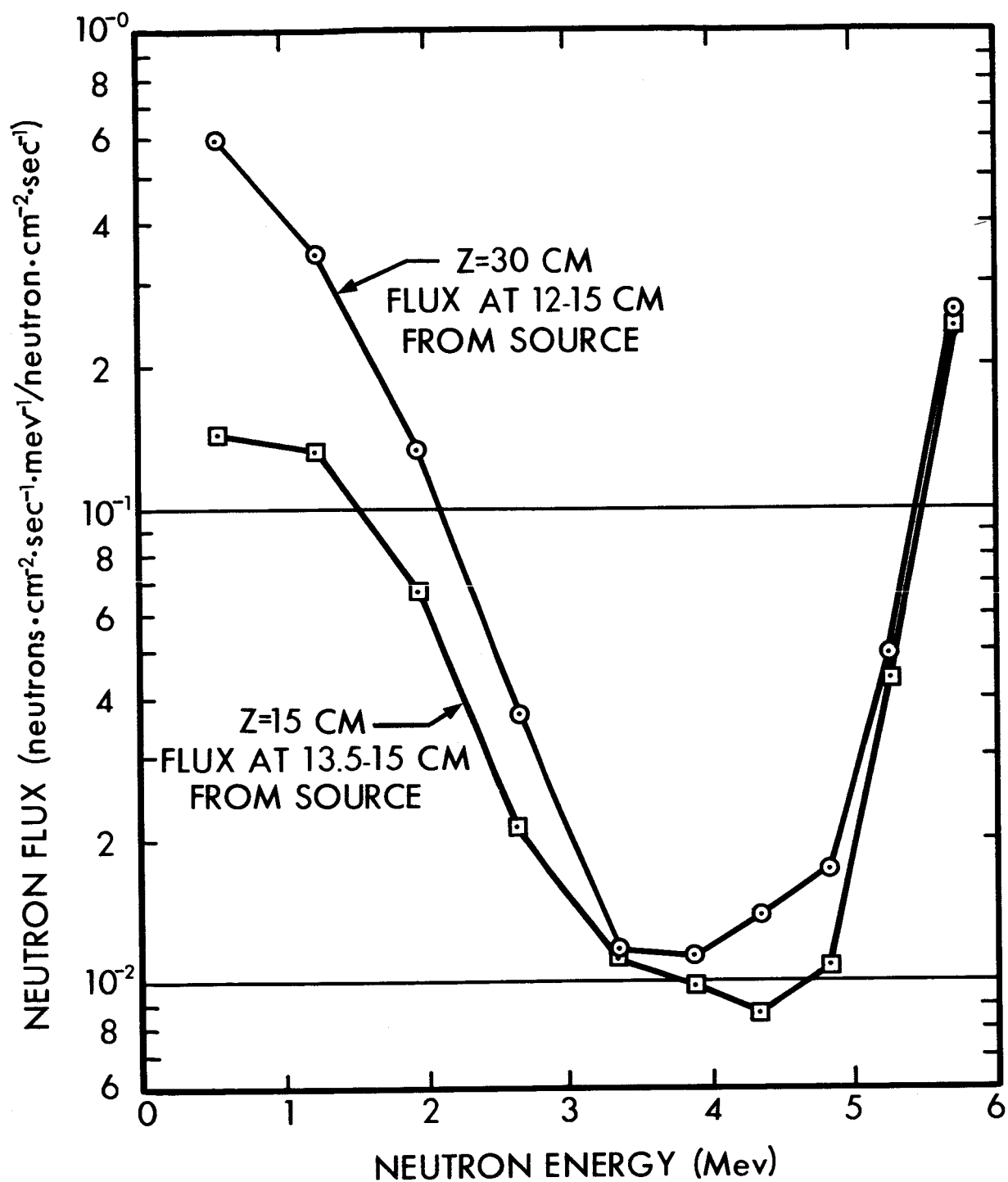


Figure 6. EFFECT OF SLAB THICKNESS ON THE NEUTRON FLUX AT A DISTANCE OF 12 TO 15 CM FROM A 6 MeV PLANE ISOTROPIC SOURCE LOCATED AT 0.01Z CM INSIDE SLABS

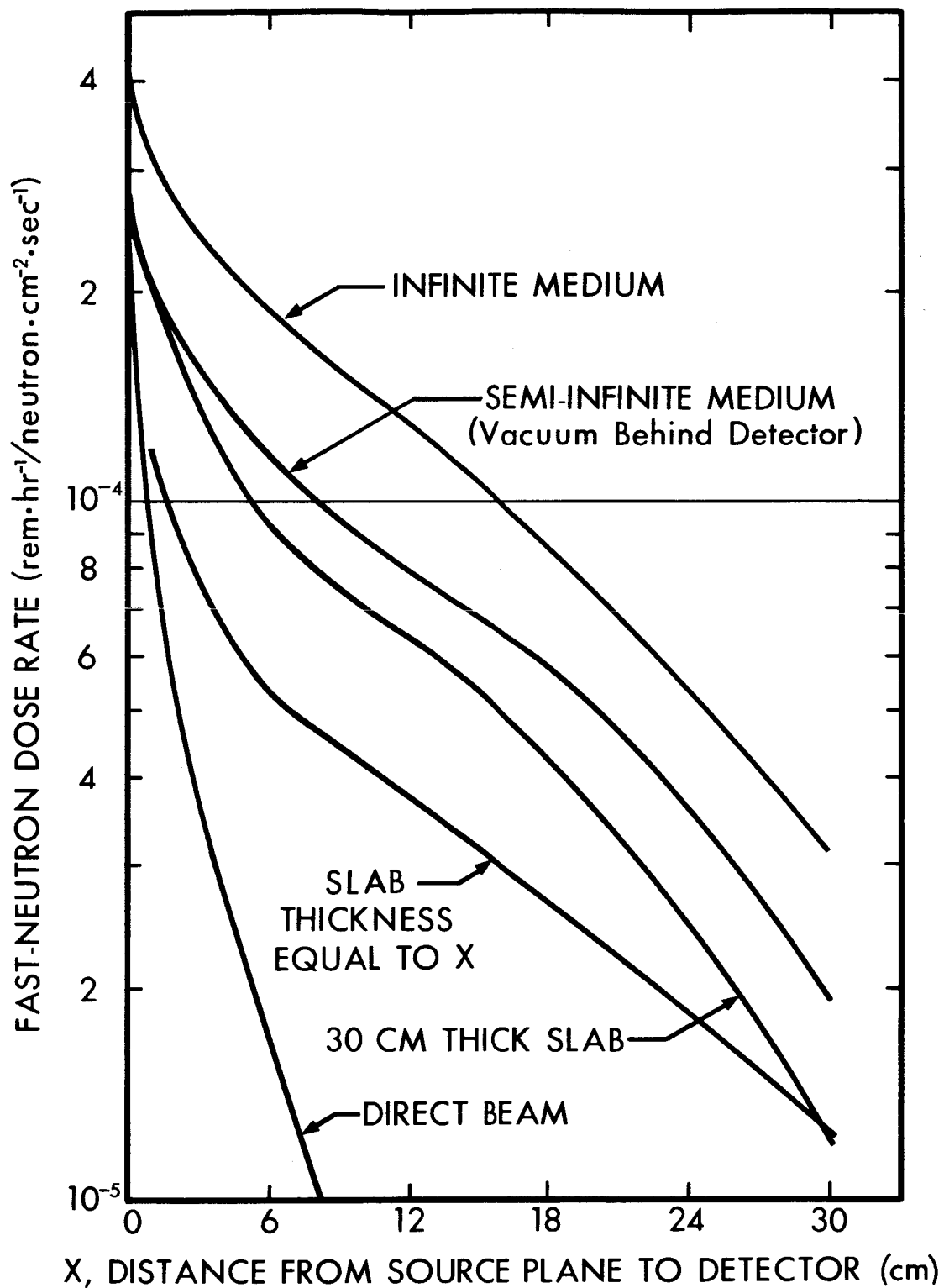


Figure 7. COMPARISON OF CALCULATIONS FOR SLAB, INFINITE MEDIUM AND SEMI-INFINITE MEDIUM GEOMETRIES: 6 Mev PLANE ISOTROPIC SOURCES IN ALUMINUM

infinite medium case is about a factor of 1.5 greater than that computed for a semi-infinite medium. Although there is a difference in magnitude between the two calculations, they both fall off with distance from the source plane at about the same rate. These results indicate that approximately 33 percent of the dose rates in an infinite medium of aluminum is contributed by neutrons undergoing collisions in the aluminum beyond a plane through the detectors.

The results obtained from the slab problems for the case where the source position is varied within a 30 cm thick aluminum slab and for the case where the source location is 0.01X cm inside slabs whose thicknesses are varied from 0 to 30 cm are also shown in Figure 7. The difference between these two curves shows the effect of the (30-X) cm of aluminum lying behind the source plane on the transmitted dose rate.

For source positions near the exit face, small values of X, there should be little difference between the transmitted fast-neutron dose rates for the 30 cm thick slab and the semi-infinite medium case. As X increases, the value of (30-X) decreases and the transmitted dose rate resulting from neutrons back scattering from the material lying behind the source plane decreases. As a result, the two curves giving the dose rate transmitted through a 30 cm thick slab and a semi-infinite medium as a function of distance from the source plane will spread apart with increasing X. Some of the difference noted between the two curves at large X could possibly result from the smoothing by eye of the calculated angular distribution of dose rates as a function of distance from a point isotropic source in an infinite medium of aluminum. These smoothed data were used in determining the modifications made to the kernel $G(R, E_0)$ to obtain the kernel $G'(R, E_0)$ which was used in calculating the semi-infinite medium dose rates.

The dose rate curves shown in Figure 7 for a slab of 30 cm in thickness

and for slab thicknesses equal to X represent the envelopes of the calculated transmitted dose rates for a 6 Mev plane isotropic source as a function of slab thickness and source position. The direct beam dose rate as a function of distance from the source plane is shown in Figure 7 to illustrate the fact that dose rate buildup factors for each of the various calculations shown in Figure 7 will differ significantly.

A better understanding of the effects of the boundaries of a slab on the transmitted dose rate can be obtained from comparisons of the calculated spatial distribution of the dose rate within a slab with that calculated for both infinite and semi-infinite media. The spatial distribution of the dose rate within a 30 cm thick aluminum slab for a 6 Mev plane isotropic source located 11.7 cm inside the slab is shown in Figure 8. The spatial distribution of the dose rate from a 6 Mev plane isotropic source in an infinite medium of aluminum is also shown for comparison with the slab results. It is seen that the slab dose rates drop below the infinite medium results at distances from the source plane that are within 10 cm of each of the slab boundaries.

The spatial distribution of the dose rate from a plane isotropic 6 Mev source located 6.3 cm from one of the boundaries of a 30 cm thick slab of aluminum is shown in Figure 9. The spatial distribution of the infinite medium dose rate is shown in the figure for comparison with the slab results. Since the source is only 6.3 cm from a boundary of the slab, the slab boundary at 30 cm effects mainly the dose in the slab for distances into the slab of from ~ 15 to 30 cm. For distances into the slab of between 0 and 15 cm, the effect of the boundary at 0 cm is to reduce the slab dose rate below the infinite medium dose rate. The dose rates at each boundary for the 30 cm thick slab case are approximately a factor of two below that computed for an infinite medium.

The spatial distribution of the dose rate within a 30 cm thick slab for

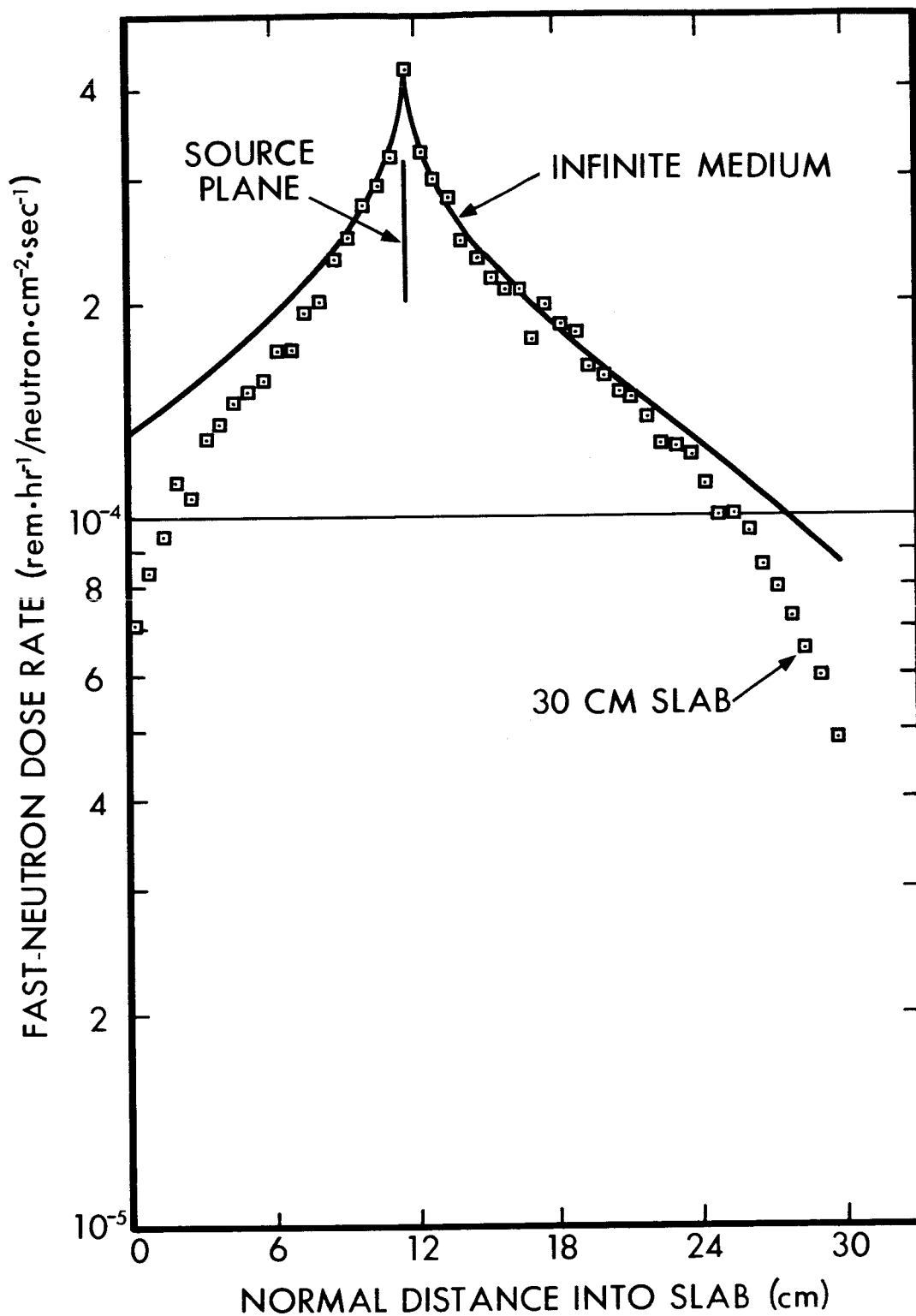


Figure 8. COMPARISON OF CALCULATIONS OF THE FAST-NEUTRON DOSE RATE SPATIAL DISTRIBUTION IN A 30 CM ALUMINUM SLAB WITH INFINITE MEDIUM CALCULATIONS: 6 Mev PLANE ISOTROPIC SOURCE LOCATED 11.7 CM FROM SLAB BOUNDARY

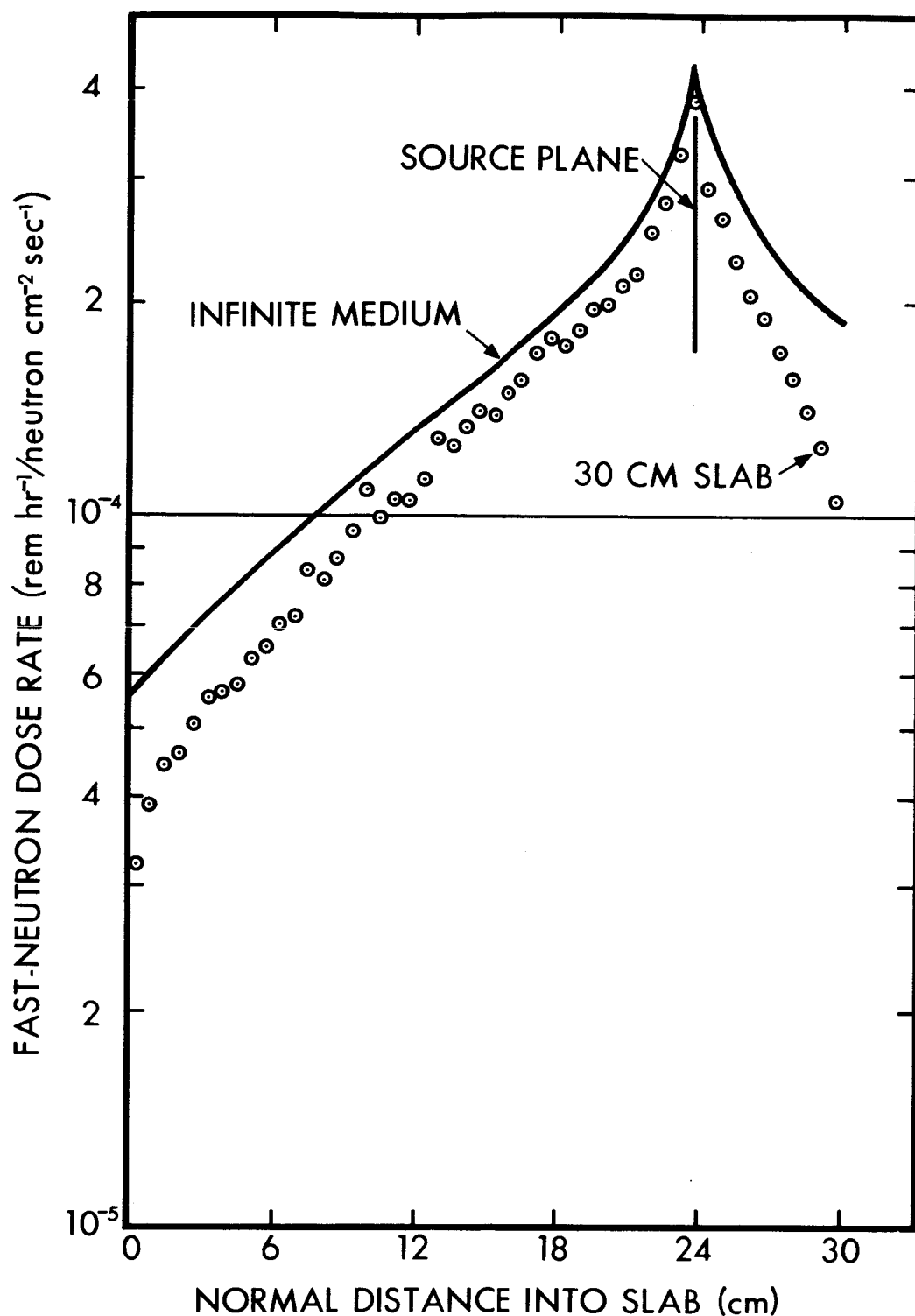


Figure 9. COMPARISON OF CALCULATIONS OF THE FAST-NEUTRON DOSE RATE SPATIAL DISTRIBUTION IN A 30 CM ALUMINUM SLAB WITH INFINITE MEDIUM CALCULATIONS 6 Mev PLANE ISOTROPIC SOURCE LOCATED 23.7 CM FROM SLAB BOUNDARY

a 6 Mev plane isotropic source located 0.3 cm from one face of the slab is shown in Figure 10. As the distance X between the source plane and detector plane increases, the thickness of aluminum beyond the detector plane decreases. For distances from the source plane of from 0 to 20 cm one would not expect the boundary at $X=30$ cm to have much effect on the spatial distribution of the dose rate in the 30 cm thick slab.

The data shown in Figure 10 for a 30 cm thick aluminum slab are also compared in the figure with the spatial distribution of the dose rate for a semi-infinite medium. In the 30 cm thick slab case there is a vacuum to the right of the aluminum slab for $X > 30$ cm as well as to the left of the source plane. In the semi-infinite medium case there is a vacuum beyond the detector plane. The two calculations are seen to be in agreement for distances of up to 20 cm from the source plane. At the source plane the two calculations should give the same result. The agreement for distances of up to 20 cm from the source plane indicates that the effect of a vacuum to the left of the 30 cm thick slab is approximately the same as the effect of the vacuum to the right of the detector plane in the semi-infinite medium case. As the distance X from the source plane in the 30 cm thick slab case becomes greater than 20 cm, the effect of both boundaries on the dose is to reduce the slab dose rates below the semi-infinite medium dose rates.

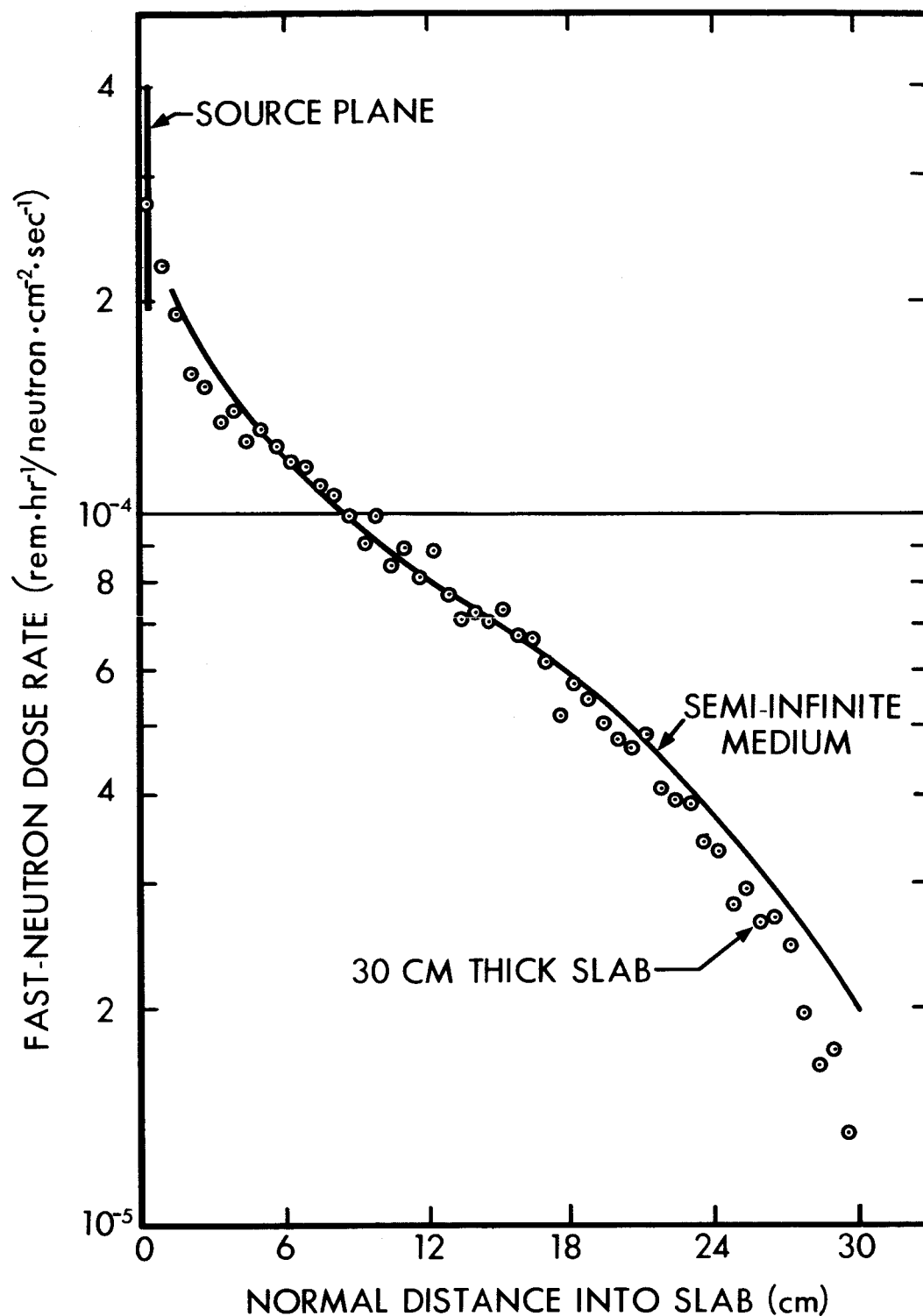


Figure 10. COMPARISON OF CALCULATIONS OF THE FAST-NEUTRON DOSE RATE SPATIAL DISTRIBUTION IN A 30 CM ALUMINUM SLAB WITH SEMI-INFINITE MEDIUM CALCULATIONS: 6 Mev PLANE ISOTROPIC SOURCE LOCATED 0.3 CM FROM SLAB BOUNDARY

CONCLUSIONS

The results presented in Figures 1 through 10 are typical of those obtained for aluminum as a function of source energy, source location, and slab thickness. The calculated dose rates within aluminum slab shields for cases where the source plane is located at least 10 cm from a slab boundary are in good agreement with the calculated infinite medium dose rates.

The effect of both of the slab boundaries on the dose rate transmitted through aluminum varies with the source location. The effects of these boundaries appear separable only when the source is located at least 10 cm from one of the slab boundaries.

The magnitude of the transmitted fast-neutron dose rate for aluminum slab shields is seen to be highly dependent on the source location within the slab as well as on the slab thickness. When the neutron source is located at one of the slab boundaries, then the shape of the transmitted fast-neutron dose rate angular distributions as a function of slab thickness appears to have reached an equilibrium for slab thicknesses greater than ~ 10 cm. For a given source-detector distance, the shape of the angular distribution of the transmitted fast-neutron dose rate does not appear to change with slab thickness, but the magnitude of the dose rates increases with increasing slab thickness up to slab thickness of about 10 cm larger than the source-detector distance. There is no increase noted in the dose rate for larger slab thicknesses.

The data presented in this paper shows that considerable error could be introduced into a machine calculation of the fast-neutron dose resulting from proton-induced nuclear evaporation in a space vehicle shield by the use of dose rate transmission factors obtained from calculations for a plane isotropic source

ACKNOWLEDGMENT

The author wishes to acknowledge the contributions of J. M. Newell to this work in the preparation of the Monte Carlo problem data and in the analysis of the results.

in either an infinite medium or a semi-infinite medium of aluminum.

Calculations similar to those described in this paper are also being made for polyethylene, carbon, and iron. The results from these calculations as well as those described above for aluminum are being compiled in a form which will be convenient for application in further machine calculations.

REFERENCES

1. Krumbein, A. D., Summary of NDA Unclassified Results of Moments Calculations for the Penetration of Neutrons Through Various Materials, Nuclear Development Corporation of America Report NDA 92-2, August 1957.
2. Allen, F. J., Futter, A., and Wright, W., Neutron Reflection and Flux Versus Depth For Concrete, BRL Report No. 1189, 1963.
3. Allen, F. J., Futter, A., and Wright, W., Neutron Reflection and Flux Versus Depth For Iron, BRL Report No. 1199, 1963.
4. Allen, F. J., Futter, A., and Wright, W., Neutron Reflection and Flux Versus Depth For Water, BRL Report No. 1204, 1963.
5. Burrell, M. O., and Cribbs, D. L., A Monte Carlo Calculation of Neutron Penetration Through Iron Slabs, Lockheed-Georgia Company Report NR-82, Vol. III, 1960.
6. Wells, M. B., Radiation Resistant Combat Vehicle Investigation-Final Report, Volume III: Monte Carlo Multilayer Slab Geometry Shielding Code C-18, General Dynamics/Fort Worth Report FZK-134-3, December 1961.
7. Wells, M. B., Monte Carlo Calculations of Fast Neutron Energy Spectra, Convair-Fort Worth Report FZM-1267, Dec. 1958 (Paper Presented at the Sixth ANP Shielding Information Meeting, 2-3 December 1958).
8. Troubetzkoy, E. S., Fast Neutron Cross Sections of Iron, Silicon Aluminum, and Oxygen, Nuclear Development Corporation of America Report NDA 2111-3, November 1959.
9. Tralli, N., et al., Neutron Cross Sections For Titanium, Potassium, Magnesium, Nitrogen, Aluminum, Silicon, Sodium, Oxygen, and Manganese, United Nuclear Corporation Report UNC-5002, January 1962.
10. Henderson, B. J., Conversion of Neutron or Gamma Ray Flux to Absorbed Dose Rate, General Electric Company Report XDC 59-8-179, August 1959.